Electron paramagnetic resonance of low-spin Mn^{2+} in RuS_2 and $RuSe_2$

Electron paramagnetic resonance of low-spin Mn²⁺ in RuS₂ and RuSe₂

Yu Jiang-Tsu[†], Huang Ying-Sheng[‡] and Lin Shoei-Sheng[‡][§]

† Institute of Physics, National Taiwan Normal University, Taipei 11718, Taiwan, Republic of China
‡ Department of Electronic Engineering, National Taiwan Institute of Technology, Taipei 10772, Taiwan, Republic of China

Abstract. Electron paramagnetic resonance (EPR) of the pyrite-structure RuS₂ and RuSe₂ doped with Mn indicates that the Mn²⁺ is in the $S = \frac{1}{2}$ low-spin state. The $g_\perp$-value is 2.135 ± 0.001 and the ^{55}Mn hyperfine constant is $81.0 \pm 2.0 \times 10^{-4}$ cm^{-1} for the Mn²⁺ in RuS₂. Slightly different values were obtained for the Mn²⁺ in RuSe₂.

1. Introduction

RuS₂ and RuSe₂ are diamagnetic semiconductors (Hulliger 1963) crystallising in the cubic pyrite structure (Sutarno *et al* 1967, Lutz *et al* 1976). There is much recent interest in these materials because of their potential applications in technologies. We report in this paper the results of an electron paramagnetic resonance (EPR) study on RuS₂ and RuSe₂ doped with manganese. The antiferromagnetic MnS₂ and MnSe₂ (Hastings *et al* 1959) also crystallise in the pyrite structure. Moreover, Mn²⁺ in these compounds is in the $S = \frac{5}{2}$ high-spin state (Hastings *et al* 1959). Therefore, it would be interesting to investigate the electronic state of Mn²⁺ which is expected to substitute for the low-spin diamagnetic Ru²⁺ (4d⁶) in RuS₂ and RuSe₂—to see whether there is a transition from the high-spin state in MnS₂ and MnSe₂ to the $S = \frac{1}{2}$ low-spin state. To date, EPR of Mn²⁺ has been reported for the pyrite-structure compounds of FeS₂ (Srinivasan and Seehra 1982), ZnS₂ (Okada *et al* 1975) and MgTe₂ (Okada and Miyadai 1978). Mn²⁺ in these three compounds was found to be in the high-spin state.

2. Experimental details

RuS₂ and RuSe₂ doped with Mn were synthesised from the elements by heating an appropriate mixture of high-purity Ru (99.95%), S (99.999%) or Se (99.999% or 99.95%), and Mn (0.1 mol% with respect to Ru) placed inside an evacuated quartz ampoule. The powders so obtained were verified by x-ray diffraction to be in the pyrite structure. Single crystals were grown by an 'oscillating chemical vapour transport' method, by using ICl₃ as the transport agent, which has proved to be a very good method

§ Permanent address: National Yuen-Lin Institute of Technology, Hu-Wei, Yuen-Lin, Taiwan, Republic of China.
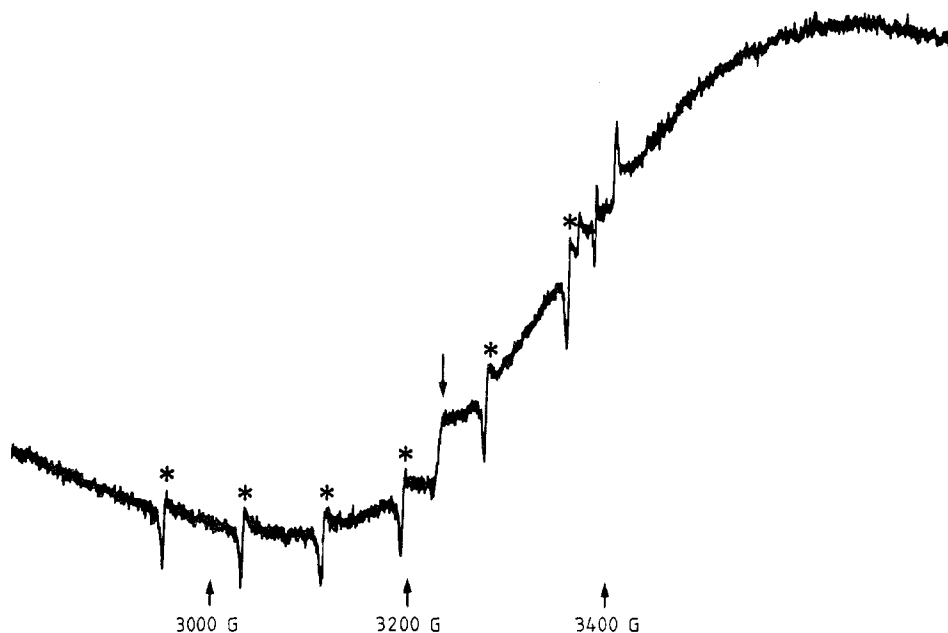
Figure 1. The EPR spectrum observed at 104 K and 9.486 GHz from a RuS_2:Mn powder sample. The six lines labelled with asterisks are the hyperfine pattern of ^{55}Mn, and the line indicated by an inverted arrow originates from an intrinsic defect related to sulphur deficiency.

for growing high-quality single crystals of RuS_2 and $RuSe_2$ (Huang and Lin 1988).

A model ER 200D EPR spectrometer equipped with low-temperature accessories by Bruker was used to investigate the subject materials. A Hewlett–Packard model 5343A counter was used to measure the microwave frequency.

3. Results and discussions

Prior to the present study on Mn-doped RuS_2 and $RuSe_2$, we have made EPR investigations of powders and single crystals of RuS_2 and $RuSe_2$ (Yu *et al* 1988). The EPR spectrum observed for these materials does not show any signal that can be construed as due to Mn^{2+}; Mn is not an impurity specified by the suppliers of the chemicals of Ru (99.95%), S (99.999%) and Se (99.999%). Figure 1 shows an EPR spectrum observed for a RuS_2 powder doped with Mn. The Mn concentration is about 0.1 mol% with respect to Ru in the starting chemicals. This spectrum was taken at 104 K at a microwave frequency of 9.4858 GHz. The six nearly evenly spaced lines (labelled with asterisks) can be construed as due to the six hyperfine lines of ^{55}Mn. This spectrum can be detected below about 170 K. The line indicated with an arrow has been observed from synthesised RuS_2 powders and RuS_2 single crystals and has been interpreted as arising from an intrinsic defect related to a deficiency in sulphur (Yu *et al* 1988). The other sharp peaks are unidentified and can be observed only for Mn-doped samples; these peaks could be related to impurities present in the Mn powder. Figure 2 shows an EPR spectrum observed from a $RuSe_2$ powder synthesised from Ru (99.95%) and Se (99.95%). Mn at a level of 50 ppm was specified as an impurity in this Se powder. This spectrum was taken at 106 K
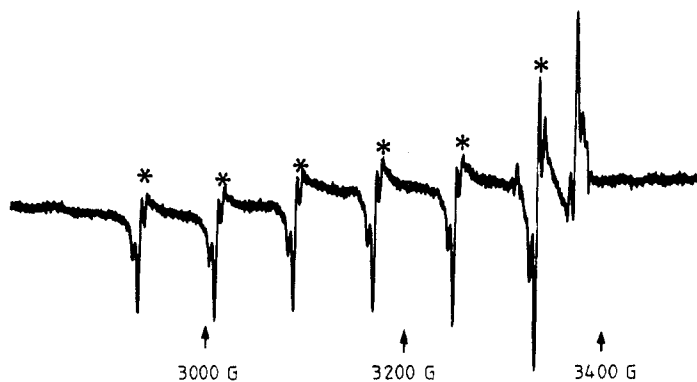
Figure 2. The EPR spectrum observed at 106 K and 9.491 GHz from a $RuSe_2$:Mn powder sample. The six lines labelled with asterisks are the hyperfine pattern of ^{55}Mn. Each Mn hyperfine line is flanked by two lines which are interpreted as the superhyperfine lines due to the ^{77}Se ($I = \frac{1}{2}$) isotope.

at a microwave frequency of 9.4906 GHz. Again, the six nearly evenly spaced lines labelled with asterisks can be regarded as the hyperfine pattern of ^{55}Mn. This spectrum can be observed below about 190 K.

Figure 2 indicates that, besides the ^{55}Mn hyperfine peaks, other peaks were present which originate from impurities present in the 99.95% pure Se powder. Besides the six ^{55}Mn peaks (each of which is flanked by two satellite lines and this will be discussed below), single structureless peaks were also observed at 1796, 5393, 6190 and 11 540 G at 150 K (not shown). The unidentified peaks just above the high-field end of the Mn hyperfine pattern (see figures 1 and 2) cannot be construed as part of the observed Mn hyperfine pattern, nor can it be explained as part of another Mn hyperfine group. It is known (Forman and Van Wyk 1966) that, when the energy of the microwave photon is nearly equal to one of the electronic zero-field splittings of an $S = \frac{5}{2}$, Mn^{2+} ion, some of the Mn hyperfine structures does not appear as six nearly equally spaced lines. This is a result of the mixing of nearly degenerate states by the off-diagonal part of the nuclear hyperfine interaction. However, we do not believe that the peaks in question can be so interpreted (an attempt to fit the observed spectrum in terms of an $S = \frac{5}{2}$ spin Hamiltonian will be discussed below).

We obtained an EPR spectrum of the Se (99.95% pure) powder used in the synthesis of the $RuSe_2$ powder at temperatures between 300 and 100 K, and the Mn^{2+} spectrum shown in figure 2 was not detected. This proves that the Mn^{2+} detected is that doped into $RuSe_2$. This assertion, which is also applicable to the Mn^{2+} spectrum observed in RuS_2 (see figure 1), is further corroborated by the observed or expected EPR spectrum of α-MnS (or α-MnSe), MnS_2 (or $MnSe_2$) and the Mn powder itself. A Lorentzian line with a g-value of 2.002 $\pm$ 0.0005 was detected from the Mn powder used in doping; the origin of the Mn^{2+} lines (see figures 1 and 2) is not unreacted Mn powder. The α-phase of MnS is a green ionic compound which is antiferromagnetic with a Néel temperature $T_N \leqslant 160$ K (Corliss *et al* 1956). The α-form is the only form of MnS that can be prepared from the elements. We prepared α-MnS by heating an equimolar mixture of Mn and S powders placed inside an evacuated quartz ampoule. The sample so obtained shows a single line with a g-value of 2.000 $\pm$ 0.0005 at 300 K. The linewidth increases and the signal amplitude decreases as the sample temperature is lowered below room temperature; this behaviour is antiferromagnetic with a Néel temperature of less than 160 K.

Therefore the Mn^{2+} spectrum under discussion does not originate from α-MnS which may possibly be present in the synthesised powders. The Mn^{2+} in both α-MnS (or α-MnSe) and the pyrite MnS_2 (or $MnSe_2$) is in the $S = \frac{5}{2}$ high-spin state and, since these compounds are ionic, consequently it is expected that the g-value should be nearly equal to the free-electron g-value. Moreover, it is known that MnS_2 cannot be prepared by heating a mixture of the elements, as it decomposes on cooling from the melt. Therefore, it can be concluded also that the spectrum under discussion cannot have originated from MnS_2 or $MnSe_2$. The other Mn compounds such as MnO, Mn_3O_4 and MnO_2 are unlikely impurities, as the samples were prepared under high vacuum (about 10^{-6} Torr). Moreover, these oxides of Mn each gives a single structureless EPR line centred around $g = 2$. The above discussion is also applicable to the broad-line spectrum (see figure 1) observed from the synthesised RuS_2: Mn powder. Neither the sharp-line Mn^{2+} spectrum nor the broad-line spectrum can be detected from the sulphur powder used in the synthesis of the RuS_2: Mn powder or from the pure RuS_2 powders. This broad-line spectrum (at 104 K) can be fitted quite well by a Lorentzian lineshape with a g-factor of 2.016. This line can be explained as arising from exchange-narrowed but dipolar-broadened Mn^{2+}. On the basis of these, we suggest that it originates from Mn^{2+} clusters (doubles, triples, etc) in RuS_2. This clustering of Mn^{2+} in RuS_2 may be compared with that in the diluted magnetic semiconductors $Cd_{1-x}Mn_xTe$ (Webb *et al* 1984, Oseroff *et al* 1980). At a concentration of about 0.01% Mn^{2+} in CdTe, a single-ion EPR spectrum of Mn^{2+} which displays electronic fine structure, Mn hyperfine structure, and Cd and Te superhyperfine structures has been observed (Lambe and Kikuchi 1960, Estle and Holton 1966). At higher concentrations of Mn in CdTe, a broad EPR line due to Mn^{2+} clusters was observed (Webb *et al* 1984, Oseroff *et al* 1980). Thus, it is very likely that the broad-line spectrum in question is due to clustered Mn^{2+} in RuS_2.

We next discuss the electronic state of the Mn^{2+} in RuS_2 and $RuSe_2$. It is known that, for the $S = \frac{5}{2}$ high-spin Mn^{2+}, the EPR spectrum is usually characterised by electronic fine structure and a g-value nearly equal to the free-electron g-value. It is also known that, for strained crystals or powders, sometimes only the $-\frac{1}{2} \rightarrow \frac{1}{2}$ electronic transition is detected by EPR. In ZnS_2 (Okada *et al* 1975), the Mn^{2+} spectrum showed a complicated fine-structure pattern, even though the sample was in powder form. Mn^{2+} in ZnS_2 showed large zero-field splittings and a g-value close to 2 (table 1); Mn^{2+} is in the high-spin state. It is also known (Dowsing and Gibson 1969) that, for high-spin $3d^5$ ions such as Fe^{3+} or Mn^{2+} in very strong ligand fields, an EPR transition can be detected only from the $S_z = \pm\frac{1}{2}$ Kramers doublet with effective g-values of $g_\parallel \simeq 2$ and $g_\perp \simeq 6$. This has been observed for Mn^{2+} in $MgTe_2$ powders (Okada and Miyadai 1978). The situation is less clear for the Mn^{2+} in polycrystalline FeS_2 (Srinivasan and Seehra 1982), although the EPR data clearly indicate that the Mn^{2+} is in the high-spin state, since the g-value is close to the free-electron g-value (see table 1). The Mn spectrum centred at 3156 G for RuS_2 or at 3154 G for $RuSe_2$ is the only Mn spectrum detected in the 0–14 kG field range. The simplicity of the spectrum suggests that it is of either cubic or axial symmetry. The model of axial symmetry is consistent with the fact that the Ru site possesses trigonal symmetry. It is known that the powder EPR spectrum is comprised of lines for which $H(\theta, \varphi)$ has a stationary value, where $H(\theta, \varphi)$ is the resonance field as a function of the polar angles of the magnetic field (Sands 1955, Kneubuhl 1960, Rubio *et al* 1979, Reynolds *et al* 1972). For an axial paramagnet with $S \geq 1$, the powder spectrum includes the parallel, the perpendicular and other peaks for which $\partial H/\partial \theta = \partial H/\partial \varphi = 0$. It is also known that in the powder spectrum the perpendicular lines show up as double peaks (up and down) in a first-derivative mode of detection, whereas the parallel lines show up as single peaks

Table 1. The g-value and the ^{55}Mn hyperfine constant observed for Mn^{2+} in RuS_2 and $RuSe_2$ powder.

Host	g	Electronic state	A^{55} $(10^{-4}\,cm^{-1})$	Reference
RuS_2	$g_\perp = 2.135 \pm 0.001$ $g_\parallel < 0.5$	Low spin	81.0 ± 1.0	This work
$RuSe_2$	$g_\perp = 2.149 \pm 0.001$ $g_\parallel < 0.5$	Low spin	80.4 ± 1.0	This work
ZnS_2	$g = 2.009 \pm 0.004$	High spin	71	Okada *et al* (1975)
$MgTe_2$	$g = 2.015 \pm 0.010$	High spin	63 ± 1	Okada and Miyadai (1978)
FeS_2	$g = 2.000 \pm 0.001$	High spin	95 ± 0.5	Srinivasan and Seehra (1982)

(up or down). The Mn spectrum shown in figures 1 and 2 corresponds to the perpendicular part of the powder spectrum.

The apparent g-factor for the Mn spectrum in question deviates very significantly from $g = 2$; consequently, if this Mn spectrum were of the $S = \frac{5}{2}$ high-spin Mn^{2+} variety, then its zero-field splittings are large compared with the energy of the microwave photon, for otherwise the apparent g-factor should be nearly equal to 2. For an $S = \frac{5}{2}$ ion in strong axial crystal fields, the effective spin Hamiltonian can be written as (Forman and Van Wyk 1966)

$$\mathscr{H} = \beta(g_\parallel H_z S_z + g_\perp H_x S_x + g_\perp H_y S_y) + A S_z I_z + B(S_x I_x + S_y I_y)$$
$$+ D[S_z^2 - S(S+1)/3] + (F/180)[35 S_z^4 - 30 S(S+1) S_z^2 + 25 S_z^2$$
$$- 6 S(S+1) + 3 S^2 (S+1)^2]. \tag{1}$$

This spin Hamiltonian is applicable to the cases wherein the deviation from cubic symmetry is large such that the cubic crystal-field term can be neglected. In such cases, it is usually found that the F-term in equation (1) is much smaller than the D-term (Forman and Van Wyk 1966). If we assume that the Mn spectrum in question is of $S = \frac{5}{2}$ and that $g \simeq 2.0$ and $F \simeq 0$, then, to fit the observed spectrum (at a frequency of 9.4958 GHz) for RuS_2, it is found that $D/g_\perp \beta = 1775$ G. The calculated energy level splittings for the field perpendicular to the symmetry axis, by using these spin-Hamiltonian parameters, is shown in figure 3. This calculation indicates that, besides the observed spectrum centred at 3154 G, the perpendicular spectrum should include peaks at 111, 1404, 1615 and 7152 G. The complete powder spectrum is much more complicated than these. By changing the g-factor to 2.05, which is much larger than those normally reported for high-spin Mn^{2+}, the picture does not change significantly. For $g = 2.05$, $F = 0$, then $D/g_\perp \beta = 1902$ G, and the perpendicular spectrum should include peaks at 454, 1287, 1319, 3156 and 7330 G. By allowing non-zero values of F, the picture remains the same; theoretically it is not possible to obtain a single line at 3156 G in the 0–14 kG field range. The above considerations demonstrate clearly that the Mn spectrum in question is not of the $S = \frac{5}{2}$ Mn^{2+} variety. The EPR of Mn in other valence states has been reported but, because of short spin–lattice relaxation times, their spectrum can be detected only at very low temperatures. On the other hand, the observed g-values are consistent with the Mn^{2+} being in the $S = \frac{1}{2}$ low-spin state. The effective g-factor evaluated from the average field of the six hyperfine lines is 2.146 for the Mn^{2+} in RuS_2 and is 2.160 in $RuSe_2$.
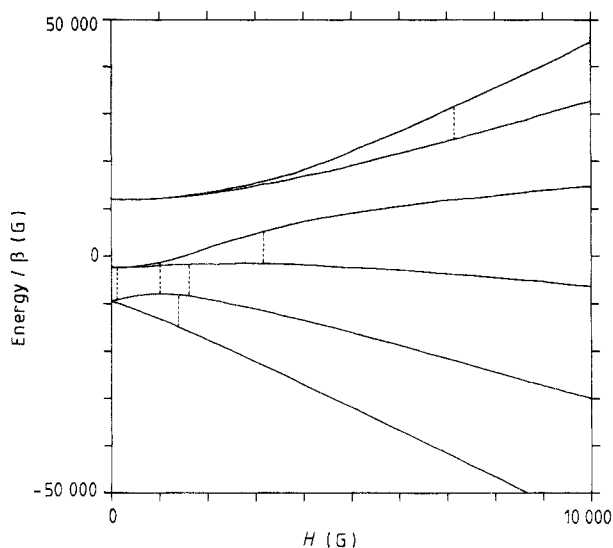
Figure 3. Energy level splittings of the $S = \frac{5}{2}$ manifold as a function of the applied magnetic field which is perpendicular to the symmetry axis of the crystal field. The spin-Hamiltonian parameters used are $g = 2$, $D/g_\perp \beta = 1775$ G and $F = 0$. The vertical arrows indicate the possible transitions at the microwave frequency of 9.4958 GHz.

The theory of the EPR of low-spin d^5 ions has been worked out by Bleaney and O'Brien (1956) and improved by Thornley (1968). For a low-spin d^5 ion in a cubic octahedral field, the g-factor of the ground state is (Raizman *et al* 1971)

$$g = (g_e + 4k)/3 \leq 2 \tag{2}$$

where $g_e \simeq 2$ is the free-electron g-value, and $k \leq 1$ is the orbital reduction factor. Low-spin Ru^{3+} ($4d^5$) in MgO gives $g = 1.8294$ (Raizman *et al* 1971). In axial or nearly axial octahedral ligand fields, the EPR spectrum is very anisotropic; $g_\| \ll 1$ and $g_\perp > 2$. Examples include low-spin Fe^{3+} and Mn^{2+} cyanide complexes (Baker *et al* 1956), $Ru^{3+}(4d^5)$ in Al_2O_3 (Geschwind and Remeika 1962), $Ir^{4+}(5d^5)$ in MgO and CaO (Raizman and Suss 1980), $Rh^{4+}(4d^5)$ and $Os^{3+}(5d^5)$ in rutile TiO_2 (Blazey and Levy 1986), and Ru^{3+} in lutetium garnets (Offenbacher *et al* 1969). The observed g-values for the Mn^{2+} in RuS_2 and $RuSe_2$ should correspond to the $g_\perp$-values. The field corresponding to the $g_\|$-value could lie outside the field range available to us (about 14 kG). The observed EPR spectrum could not be isotropic, since the observed g-value is inconsistent with the predicted and the observed values for a d^5 ion in cubic fields. Moreover, an isotropic Mn^{2+} spectrum is inconsistent with the trigonally distorted ligand field at the Ru^{2+} site. For this to happen, the unpaired electrons of Mn^{2+} would have to be spread over an impurity band within the band gap. However, the well resolved hyperfine pattern observed indicates that the unpaired electrons are very well localised at the Mn^{2+}. The unpaired electrons are localised at discrete levels within the band gap. The transition of Mn^{2+} from the high-spin state in MnS_2 and $MnSe_2$ to the low-spin state in RuS_2 and $RuSe_2$ is an interesting phenomenon, and it could have been caused by the so-called strain interaction (Ohnishi and Sugano 1981) induced by a mismatch between the ionic radii of the high-spin dopant ion and the low-spin host ion.

As can be seen from figure 2, each hyperfine line of Mn^{2+} is flanked by two satellite lines with an average splitting of 6 G. These satellite lines can be regarded as due to the superhyperfine coupling of the unpaired electrons to its neighbouring Se^{77} isotope (7.58% natural abundance and nuclear spin $I = \frac{1}{2}$). Se superhyperfine splittings with $A = 2.10 \times 10^{-4}$ cm^{-1} and $B = 2.81 \times 10^{-4}$ cm^{-1} has been observed for the tetrahedral Mn^{2+} in hexagonal ZnSe (Estle and Holton 1966). The RuX_2 (X = S, Se) is built up of Ru^{2+} and X_2^{-2} in a cubic pyrite structure. The space group of the structure is the cubic T_h^6(Pa3), and there are four molecular units in a unit cell of the lattice. The point symmetry at the Ru site is $\bar{3}$ and that at the S site is 3. The Ru–X_6 octahedron is trigonally distorted, but the six Ru–X distances are all equal, and the symmetry axis of the octahedron points along a [111] axis of the lattice. The measured average signal intensity of the two satellite peaks relative to that of the main peak is respectively 22, 22, 19, 21, 21 and 19% in order of the resonance field for the main peaks. The average value is approximately 21%, which is nearly equal to the expected value of approximately 23% for superhyperfine interactions with six equivalent Se nuclei. The highest-field main peak appears much stronger in intensity than the other five peaks (see figure 2); we speculate that this is due to an accidental superposition with an impurity peak. The sulphur superhyperfine splittings are not detected in RuS_2, and this is probably because the only natural isotope with a nuclear spin ($I = \frac{3}{2}$) is the ^{33}S isotope which is only of 0.76% abundance. The spacing between the successive hyperfine lines increases monotonically with the field, indicating higher-order perturbation corrections to the hyperfine splitting. For an $S = \frac{1}{2}$ and nuclear spin I paramagnet with axial symmetry, the resonance field perpendicular to the symmetry axis for the hyperfine lines is (Atherton 1973)

$$H = H_0 - (B/g_\perp \beta)M - [(A^2 + B^2)/4g_\perp^2 \beta^2 H_0][I(I + 1) - M^2] \qquad (3)$$

where $H_0 = h\nu/g_\perp \beta$, $I = \frac{5}{2}$ for ^{55}Mn, and A and B are the parallel and the perpendicular components of the hyperfine constant. The evaluated parameters are listed in table 1. The evaluated and the observed (in parentheses) hyperfine spacings are, for RuS_2, 79.4 G (79.6 G), 80.3 G (80.3 G), 81.2 G (81.2 G), 82.1 G (82.6 G) and 83.0 G (82.7 G). The values for $RuSe_2$ are 77.9 G (77.5 G), 79.0 G (79.0 G), 80.1 G (80.1 G), 81.2 G (81.0 G) and 82.3 G (82.1 G).

We have grown single crystals of $RuSe_2$ from the synthesised powder whose EPR spectrum is shown in figure 2. We took EPR measurements of these single crystals at temperatures between 300 and 100 K. The spectrum shown in figure 2 which originates from localised and isolated Mn^{2+} ions in the $RuSe_2$ powder cannot be detected, nor any other EPR spectrum that can be construed as due to Mn^{2+} in isolation or in aggregation. Apparently, single crystals of $RuSe_2$ doped with Mn cannot be grown by the chemical vapour transport method by using ICl_3 as the transport agent. We have also grown several single crystals of RuS_2, by using the synthesised powder (whose EPR spectrum is shown in figure 1) as the starting materials. The EPR spectra for several of these single crystals at temperatures between 300 and 100 K were obtained. The EPR spectrum shown in figure 1 is not detected. Instead, broad-line spectra were observed from these samples; this type of spectrum is absent in other RuS_2 crystals for which no Mn was added to the starting material for crystal growth. This spectrum could be due to Mn^{2+} in aggregation, except that the observed (111) rotation pattern does not show the 120° (or 60°) symmetry required of the host lattice. The origin of this spectrum is at present not understood. We have also made EPR measurements on the left-over (untransported) RuS_2:Mn powder, and the single-ion low-spin Mn^{2+} EPR spectrum shown in figure 1 was not detected; a

possible chemical reaction between Mn and the ICl_3 transport agent used in the crystal growth is indicated.

4. Conclusion

Based on g-value, the present experimental evidence is fairly conclusive that the Mn^{2+} is in the $S = \frac{1}{2}$ low-spin state in the pyrite-structure compounds of RuS_2 and $RuSe_2$, a phenomenon which is worthy of further investigations. Although the chemical vapour transport method using ICl_3 as the transport agent has been proven to be a very good method for the growth of high-quality RuS_2 and $RuSe_2$ single crystals, it is apparently not suitable to grow these crystals doped with Mn. Other methods which have been successfully used to grow these crystals may prove to be more useful.

Acknowledgments

References

Atherton N M 1973 *Electron Spin Resonance* (New York: Wiley) p 227
Baker J M, Bleaney B and Bowers K D 1956 *Proc. Phys. Soc.* B **69** 1205–15
Bleaney B and O'Brien M C M 1956 *Proc. Phys. Soc.* B **69** 1216–30
Blazey K W and Levy F 1986 *Solid State Commun.* **59** 335–8
Corliss L M, Elliott N and Hastings J M 1956 *J. Appl. Phys.* **29** 391–2
Dowsing R D and Gibson J F 1969 *J. Chem. Phys.* **50** 294–303
Estle T L and Holton W C 1966 *Phys. Rev.* **150** 159–67
Forman A and Van Wyk J A 1966 *J. Chem. Phys.* **44** 73–6
Geschwind S and Remeika J P 1962 *J. Appl. Phys., Suppl.* **33** 370–7
Hastings J, Elliott N and Corliss L M 1959 *Phys. Rev.* **115** 13–7
Hulliger F 1963 *Nature* **200** 1064–5
Huang Y S and Lin S S 1988 *Mater. Res. Bull.* **23** 277–85
Kneubuhl F K 1960 *J. Chem. Phys.* **33** 1074–8
Lambe J and Kikuchi C 1960 *Phys. Rev.* **119** 1256–60
Lutz H D, Willich P and Haeuseler H 1976 *Z. Naturf.* a **31** 847–52
Offenbacher E L, Miller I A and Kemmer G 1969 *J. Chem. Phys.* **51** 3082–6
Ohnishi S and Sugano S 1981 *J. Phys. C: Solid State Phys.* **14** 39–55
Okada O and Miyadai T 1978 *Japan. J. Appl. Phys.* **17** 231–2
Okada O, Miyadai T and Akimoto S I 1975 *J. Phys. Soc. Japan* **39** 312–6
Oseroff S B, Calvo R, Giriat W and Fisk Z 1980 *Solid State Commun.* **35** 539–42
Raizman A and Suss J T 1980 *Phys. Rev.* B **22** 1141–9
Raizman A, Suss J T and Szapiro S 1971 *Solid State Commun.* **9** 1799–801
Reynolds R W, Boatner L A, Finch C B, Chatelain A and Abraham M M 1972 *J. Chem. Phys.* **56** 5607–25
Rubio J O, Munoz E P, Boldu J O, Chen Y and Abraham M M 1979 *J. Chem. Phys.* **70** 633–8
Sands R H 1955 *Phys. Rev.* **99** 1222–6
Srinivasan G and Seehra M S 1982 *Solid State Commun.* **42** 857–9
Sutarno O, Knop O and Reid K I G 1967 *Can. J. Chem.* **45** 1391–1400
Thornley J H M 1968 *J. Phys. C: Solid State Phys.* **1** 1024–37
Webb D J, Bhagat S M and Furdyna J K 1984 *J. Appl. Phys.* **55** 2310–2
Yu J T, Lin S S and Huang Y S 1989 *J. Appl. Phys.* **65** 4230–3